***Chapter 9***
Print ISBN: 978-93-89816-52-5, eBook ISBN: 978-93-89816-53-2

# A Wide Infrared Tuning Range of the Bulk CdSe Doped with Cu Photodetector

**Hassan H. Mohammed[1*] and Salwan K. J. Al-Ani[2]**

DOI: 10.9734/bpi/taps/v4

## ABSTRACT

In this work, the adopted method of the CdSe doped with Cu (CdSe: Cu) photodetector is presented. This detector is prepared by vacuum evaporation of CdSe films on a glass substrate followed by vacuum annealing under an argon atmosphere for doping with copper. The detector is found, for the first time, to cover a wide range of the infrared besides the visible region of the electromagnetic spectrum. This finding of the wavelength tuning is due to the localized energy states of copper atoms inside the band gap of the CdSe. These characteristics stem from the unique band structure of CdSe: Cu. This tuning is compared with recent work in the corresponding colloidal CdSe-ZnS core shell quantum dots and with the quantum well (QWIR) and quantum dots infrared detectors (QDIR). The major significance of this developed detector is in its synthesis simplicity and its fabrication processes costs in comparison with that of the (QWIR) and (QDIR) detectors. The structural analysis results demonstrated that the vacuum annealing in competition with the doping concentration improves significantly the film structure. A better crystalline structure is reported at 5 wt% of Cu concentration and at annealing temperature of 350ºC. Besides the measured specific detectivity at room temperature is $D^*=2.31\times10^8$ cm $Hz^{1/2}W^{-1}$. This value approaches the detectivity of the state of art mercury cadmium telluride (MCT). This result paves the way for further investigations and improvements.

*Keywords: CdSe:Cu; photodetector; infrared; tuning range; detectivity.*

## ABBREVIATIONS

| | |
|---|---|
| *Ag* | *: Silver* |
| *AlGaN* | *: Aluminum gallium nitride* |
| *Au* | *: Gold* |
| *CdS* | *: Cadmium sulfur* |
| *CdSe* | *: Cadmium Selenide* |
| *CNC* | *: Computer numerical control machine* |
| *Cu* | *: Copper* |
| *$CO_2$* | *: Carbon dioxide* |
| *CuCl* | *: Copper chloride* |
| *CW* | *: Continuous wave* |
| *3D* | *: Three dimensional* |
| *DC* | *: Direct current* |
| *FWHM* | *: Full width at half maximum* |
| *GaAs* | *: Gallium arsenide* |
| *GaN* | *: Gallium nitride* |
| *IR* | *: Infrared* |
| *MCT* | *: Mercury cadmium telluride* |
| *MEG* | *: Multiple exciton generation* |

*[1]Department of Computer Engineering Technology, Iraq University College, Alestiqlal Street, Basrah, Iraq.*
*[2]Department of Physics, College of Science, Al-Mustansiriya University, Baghdad, Iraq.*
**Corresponding author: E-mail: dr.hassanh50@gmail.com;*

*NEP : Noise equivalent power*
*OPDs : Organic photodetectors*
*rms : Root mean square*
*SEM : Scanning electron microscope*
*QD : Quantum dot*
*QDIP : Quantum dots infrared photodetector*
*QDIR : Quantum dots infrared detectors*
*QWIR : Quantum well infrared detectors*
*XANES : X-ray absorption near edge spectroscopy*
*ZnS : Zinc sulfide*

## 1. INTRODUCTION

In the last two decades there are great potential interests in the design and implementation of photodetectors. The motivation of such interests is the expansion of absorption spectrum and increase of detectivity at room temperature. Expansion of electromagnetic spectrum provides a wide range of applications including high speed data communication Zhang et al. [1], medical diagnosis Maiti et al. [2], solar cells in the visible range Kashyout et al. [3], while the infrared (IR) detectors are used in thermal imaging, night vision, heat seekers. In the present work we have found that the bulk CdSe semiconductor material when doped with Cu impurity leads to the electromagnetic spectrum expansion. Besides, the implementation of this material as a photoconductive detector could reach a detectivity value comparable with that of the state of art mercury cadmium telluride (MCT) at room temperature. The quantum dots infrared photodetector (QDIP) have emerged as a potential alternative to MCT and QWIP [4]. Asgari and Razi [5] have designed a novel infrared quantum photodetector using a cubic shaped 6nm GaN quantum dots capped with AlGaN. The D* of this detector was calculated and found to be $3\times10^{8}$cm $Hz^{1/2}W^{-1}$at room temperature. Diedenhofen et al. [6] have demonstrated that the integration of colloidal quantum dot photodetector with color tunable plasmonicnanofocussing lenses offer a significant color selectivity. Such lenses facilitate light concentration at the nanoscale and enhance light matter-interactions. Wageh et al. [7] have prepared Cu doped CdSe quantum dots, only a broad emission band with a large Stokes shift was observed. Cakmakyapan et al. [8] have used engineered photoconductive nanostructured based on gold-patched graphene nano-strips to demonstrate improvements of the response times by more than seven orders of magnitude and an increase in bandwidth of one order of magnitude compared to those of higher responsivity grapheme photodetectors based on quantum dots and tunneling barriers. Yang and Ma [9] have reviewed the development of organic semiconductor photodetectors (OPDs), and they demonstrated their advantages over inorganic semiconductors. They concluded that OPDs have not yet practically applied. One possible reason is that the overall performance of organic photodetectors is still inferior to that of inorganic photodetectors, and the advantages of OPDs such as flexibility, large area, and low cost are not fully exhibited. Recently, organic- inorganic hybrid perovskite materials [10] attracted considerable research interests owing to their bandgap, long-range electron and hole transport lengths and high absorption coefficients. These unique features render perovskites electrical and optoelectronic properties for optoelectronic devices. The aim of the present work is to investigate an alternative approach for wavelength tuning extending from the visible to the IR spectrum region. For this purpose, we focus in particular on the CdSe doped with different concentrations of Cu atoms in which photoconductive detector plays a major role. This detector has found for the first time to cover a wide spectral range and operating at roomtemperature, besides its preparation simplicity and lower costs than any other types of photodetectors mentioned earlier.

## 2. PHOTODETECTORS FIGURES OF MERIT

To describe the performance of a photodetector under specified conditions, and make a meaningful comparison of sensitivity of quite different detectors, it is essential to have an in- depth understanding of their figures of merit [11]. One of the important figures of merit is the signal-to-noise ratio. Another commonly used figures of merit is the noise equivalent power (NEP) which is defined as the root mean square value of the sinusoidal modulated radiant power incident on the photodetector generating a signal output equal to the root mean square (rms) noise output from the detector. A convenient way to characterize the sensitivity of infrared detector is to specify its NEP. The most used

figures of merit is the specified detectivity D* which is defined as

$$D^* = (A\,\Delta f)^{1/2} / NEP \quad (1)$$

Where A is the photodetector area, and Δf is the bandwidth, the reference bandwidth is always 1 Hz. The units of D* are cm $Hz^{1/2}$ $W^{-1}$. The importance of D* is that this figure of merit permits comparison of detectors of the same type, but having different areas.

The performance of photoconductor in particular is measured in terms of two parameters: the photoconductivity gain and the response time of the detector. The photoconductivity gain is defined as the numbers of charge carriers which pass between the contact electrodes per second for each photon absorbed per second

$$Gain = \Delta I / q\, G_{pair} \quad (2)$$

Where ΔI is the photocurrent in ampers, q is the electron charge and $G_{pair}$ is the total number of electron-hole pairs created in the photoconductor per second by the absorption of light. The gain may be expressed as the ratio of the lifetime of a free carrier to the transit time for that carrier, i.e the time required for the carrier to move between the electrodes. For a semiconductor in which one- carrier conductivity dominates,

$$Gain = \tau / t_r = \tau\, \mu\, V / L^2 \quad (3)$$

Where τ is the lifetime of a free carrier, $t_r$ the transit time for this carrier, μ the mobility, V the applied voltage, and L the electrode spacing. The gain is thus dependent upon the lifetime of the free carriers as a critical parameter.

The responsivity parameter R reflects the gain of the detector and is defined as the output signal (typically voltage or current) of the detector produced in response to a given incident radiant power falling on the detector

$$R_v = V_s / P_0 \quad \text{or} \quad R_i = I_s / P_0 \quad (4)$$

Where $V_s$ is the output voltage (V), $I_s$is the output current (A), and $P_0$ is the radiant input power (W). Although responsivity provides a good indication about the performance of an infrared detector, it does not take into account the level of any intrinsic noise in the device and, therefore, provides little or no information about the threshold sensitivity of the detector. The NEP can be related to the detector responsivity, $R_v$and $R_i$, and the rms detector noise [12].

$$NEP = V_n / R_v \quad \text{or} \quad NEP = I_n / R_i \quad (5)$$

Where $V_n$ or $I_n$ is the rms noise voltage (current displacement) measured within the whole operation bandwidth. Eq. (1) can be written as

$$D^* = (A\,\Delta f)^{1/2} R_v / V_n \quad \text{or} \quad D^* = (A\,\Delta f)^{1/2} R_i / I_n \quad (6)$$

Normalized (or specific) detectivity D* is, therefore, the detector output signal-to- noise ratio at 1 Watt of input infrared radiation normalized to a detector with a unit active area and a unit bandwidth.

## 3. EXPERIMENT

Thin films of CdSe (purity= 99.999%) are prepared by vacuum evaporation on a glass substrate (7.6×2.6 $cm^2$) using Balzers-OE-8 evaporation unit (vacuum pressure $10^{-8}$torr). High purity (99.999%) aluminum is deposited on the CdSe film to act as ohmic contacts. Copper atoms of a different weight percentage are also introduced into the CdSe lattice by dipping the films in a CuCl solution, complemented by annealing using a vacuum furnace and flowing argon gas. The experimental layout is shown in Fig. 1. The sample is annealed at variable temperature between 100 and 350ºC for a

period of 2.5 hours. It has been found that a better film structure was obtained at the temperature of 350ºC. The doped CdSe films prepared by this method have enjoyed characteristics similar to the CdSe single crystal doped with impurity atoms. The mask was fabricated from Mo material using a CNC cutting machine. The shape and dimensions of the mask are given in Fig. 2. The photocurrent and spectral response were measured by the detector test bench DSR-500 supplied by Optronic laboratories. For lasers wavelength response test, the mounted test bench shown in Fig. 3a was used. This test bench consists of the laser source, mechanical chopper for chopping the CW $CO_2$ laser, CdSe: Cu detector and storage oscilloscope. The detector bias circuit is shown in Fig. 3b which presents a DC power supply (100V, 5 mA) and a load resistor. In the present experiment a bias voltage of 20V was used. For responsivity measurements, the power incident on the detector area is measured by a calibratedthermopile.

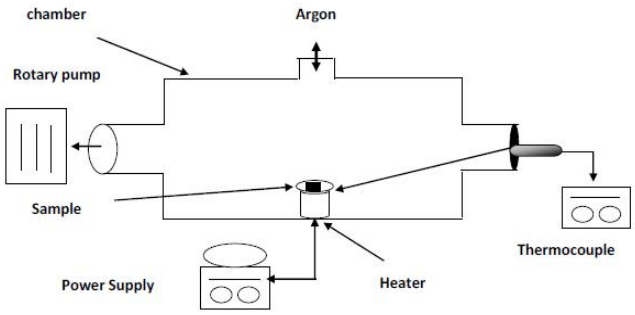


**Fig. 1. Film annealing**

**Fig. 2. The detector mask**

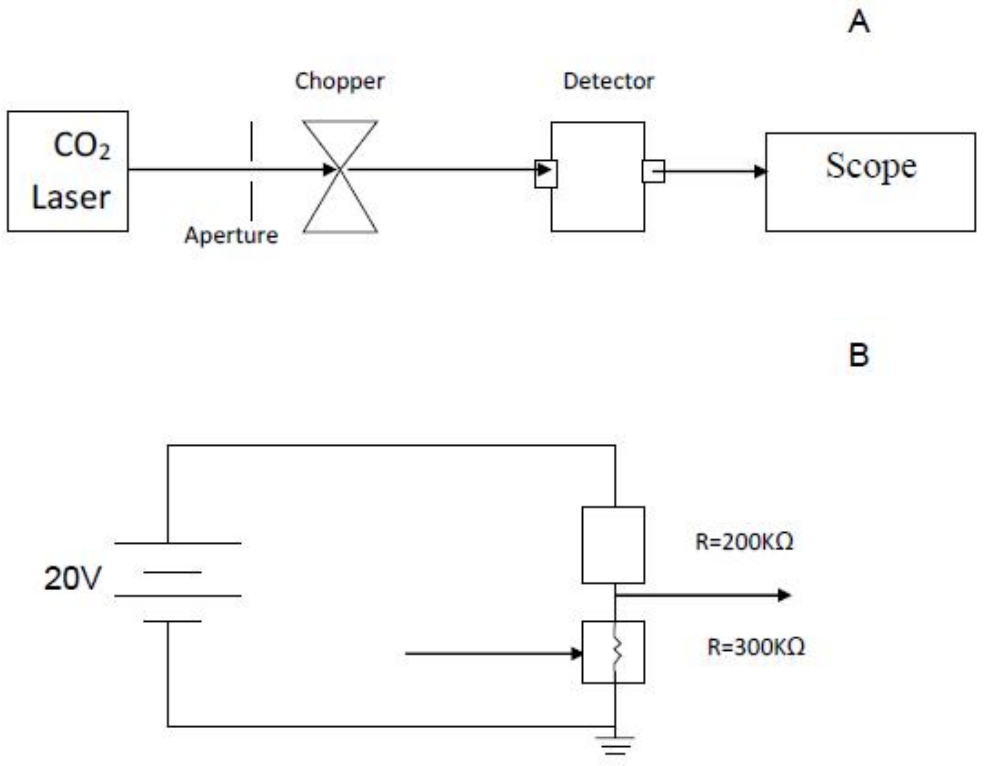


**Fig. 3. (A) Detector response test bench, (B) Detector bias circuit**

## 4. RESULTS AND DISCUSSION

### 4.1 Structural Properties

The doping of pure CdSe with Cu at different concentrations (film thickness= 1µm) improves significantly the structure. Better crystalline is reported at 5wt% Cu concentration. The X-ray diffraction of Cu doped samples depicts that only reflection from the (100) plane appeared and indicated that a single crystal grew on this plane. Fig. 4 shows the diffraction pattern of CdSe doped with 5 wt% of Cu and at 2wt% for comparison. The results of the X-ray diffraction pattern are confirmed by the SEM morphology which indicates the single crystalline with hexagonal (wartzite) of the film structure at 5wt% of doping (Fig. 5).This large crystalline structure change with doping indicates the incorporation of this dopant within substitusional or interstitial site in the CdSe lattice structure. It was shown that the grain size increases from 0.4µm to 2.87µm with an increase in Cu concentrations (Fig. 6). A great improvement of the films structures was achieved at doping with 5wt% of Cu complemented by 2.5 hours of annealing at 350ºC. The improvement in the crystal structure leads to a better optical sensitivity than that found in the case of the pure CdSe. The crystal structure is found to be hexagonal and cubic when Cu concentrations are below 3wt%. The increase in grain size can be related to the atoms thermal energy gained by annealing in presence of argon gas which facilitates the recrystallization. The SEM morphology results of CdSe:Cu (5wt% of Cu) and the X-ray diffraction of the same material can be considered to be identical [13].

### 4.2 Gain Coefficient and Responsivity

The gain coefficient is $G = I_p/I_d$ , the photocurrent to dark current ratio for CdSe and CdSe doped with Cu (1, 2, 3 and 5 wt%). Fig. 7 shows the measured *G* value as a function of wavelength for the cases of 3 and 5 wt% of Cu. The maximum *G* value obtained in the present work was $8.87xl0^3$ with an illuminance of 1000 Lux and bias V= 10 V, which is higher than the corresponding *G* value for pure CdSe by 25 times. Further, the value of *G* obtained here is much higher than values published by others. However, a value of G= 60 was obtained by Glew [14] for CdSe prepared by the sputtering method, while Metha and Sharama [15] obtained G= 300 for a Shottky-type CdSe. For a CdSe single crystal [16] a value of $G=2x10^3$ has been obtained. The higher gain value reported in the present work for CdSe:Cu compared to that published by others can be explained in terms of the cross section of holes and electrons. The Cu atoms possess a trapping cross section for holes which is relatively greater than that for electrons ($\sigma_p/\sigma_n= 10^5$) which clearly indicates that the Cu centers act as a photoconductivity sensitizer [17]. This is not surprising since it also acts as a sensitizing center in a similar semiconductor CdS [18]. It is clear from Fig. 7 that an additional peak but well resolved structure appears in the high- energy region.

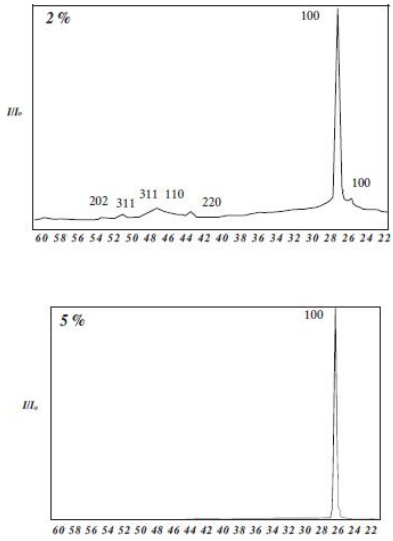


**Fig. 4. The diffraction pattern of CdSe doped with 5 wt% of Cu and 2 wt%**

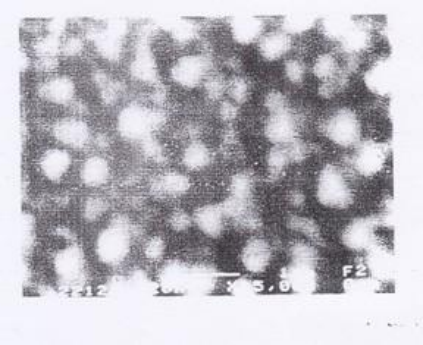

**Fig. 5. SEM morphology of CdSe doped with Cu at 5 wt% concentration**

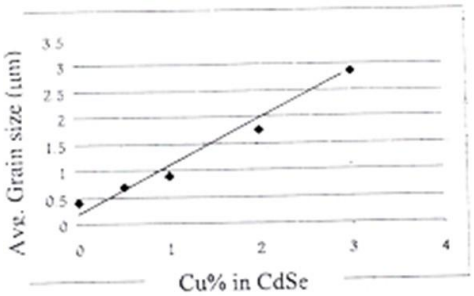


**Fig. 6. The average grain size as a function of Cu concentration**

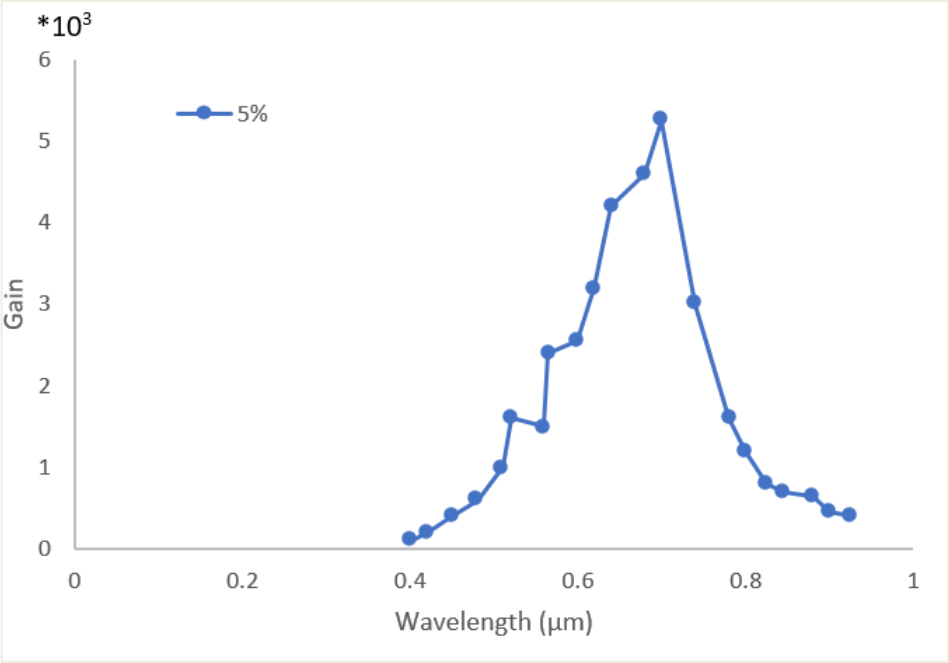


**Fig. 7. Gain coefficients versus wavelength for CdSe doped with 5 wt% of Cu**

The peaks are located at 2.34 and 2.21 eV, which means at 0.63 and 0.5 eV lines below the top of the valence band. Such peaks correspond to 3D transition of Cu from deep levels in the valence band (Barreto et al. 1987). Such levels are formed due to the interaction between metal contacts and the semiconductor surface. The peaks are not clearly resolved in the responsivity and quantum efficiency measurements as shown in Figs. 8 and 9, respectively. However, it is observed that the continuum spectral response in the region between 0.5 and 0.65 eV, which gives further and clear evidence for the existence of deep Cu levels below the top of the valence band of CdSe [19].

### 4.3 The Optical Properties

The absorption coefficient increases with the increase in the Cu doping concentration (Fig. 10). Red shift in photon energy was found to be relative to the pure CdSe. This shift can be related to the presence of localized Cu levels inside the band gap of CdSe. The Cu levels induced field effect that shift the band edge towards energy lower than that of the pure CdSe. The change in the absorption coefficient $\Delta\alpha = (\alpha_{doped} - \alpha_{pure})$ was calculated for various doping concentrations. Fig. 11 depicts the

values of Δα as a function of photon energies (hf). Δα represents the electronic transitions for various copper levels inside the band gap to the conduction band. The positions of the copper levels were estimated from the full width at Maximum (FWHM) for each doping concentrations. As predicted by Wei et al. [20], the CdSe can easily be n-doping in consistent with observation of deep levels below the conduction band minimum. These levels were localized relative to the conduction band at (0.67, 0.825 and 1.1 eV) corresponding to the Cu concentrations (1, 2 and 5 wt% respectively). Other levels were detected in the near and mid infrared region of the spectrum. The first level is situated at 0.116eV just below the conduction band. The position of this level is accurately ascertained when CdSe: Cu detector is selectively excited by a modulated $CO_2$ laser (10.6 μm), and the output signal was detected by the storage oscilloscope (Fig. 12). Another accurate determination of Cu level is by selective excitation using the GaAs semiconductor laser pulse. This pulse is shown in Fig. 13 with a rise time of 0.2 μs.

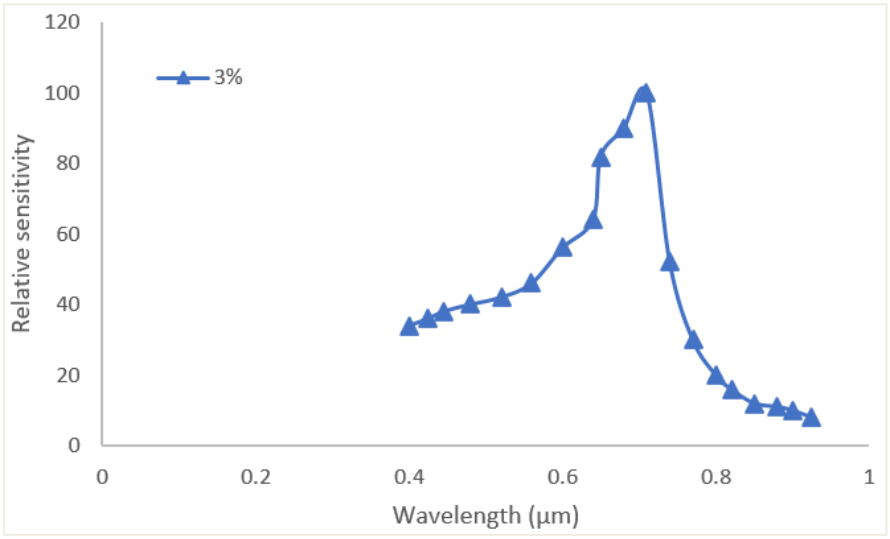


**Fig. 8. Spectral response for the CdSe:Cu detector at 3 wt% of Cu**

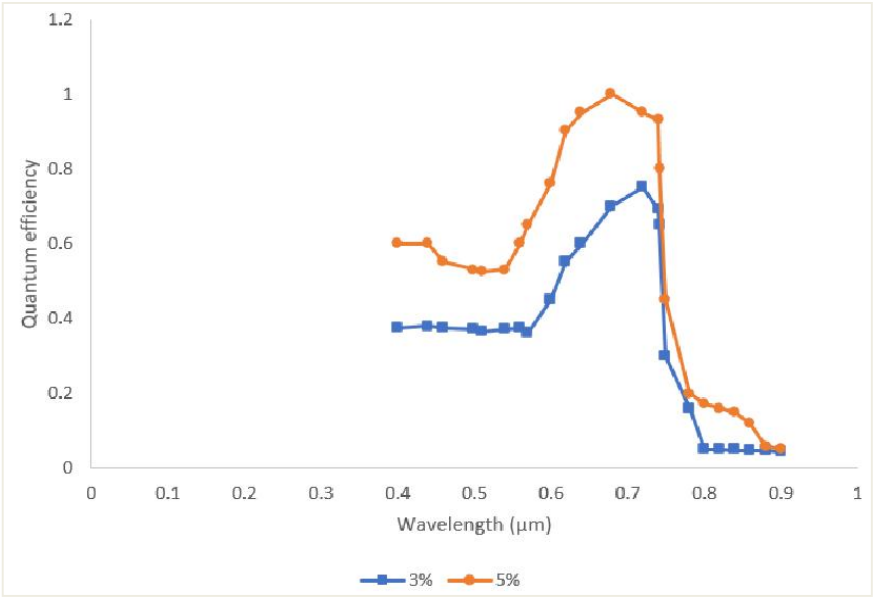


**Fig. 9. Quantum efficiency of the CdSe:Cu detector at 3 and 5 wt% of Cu**

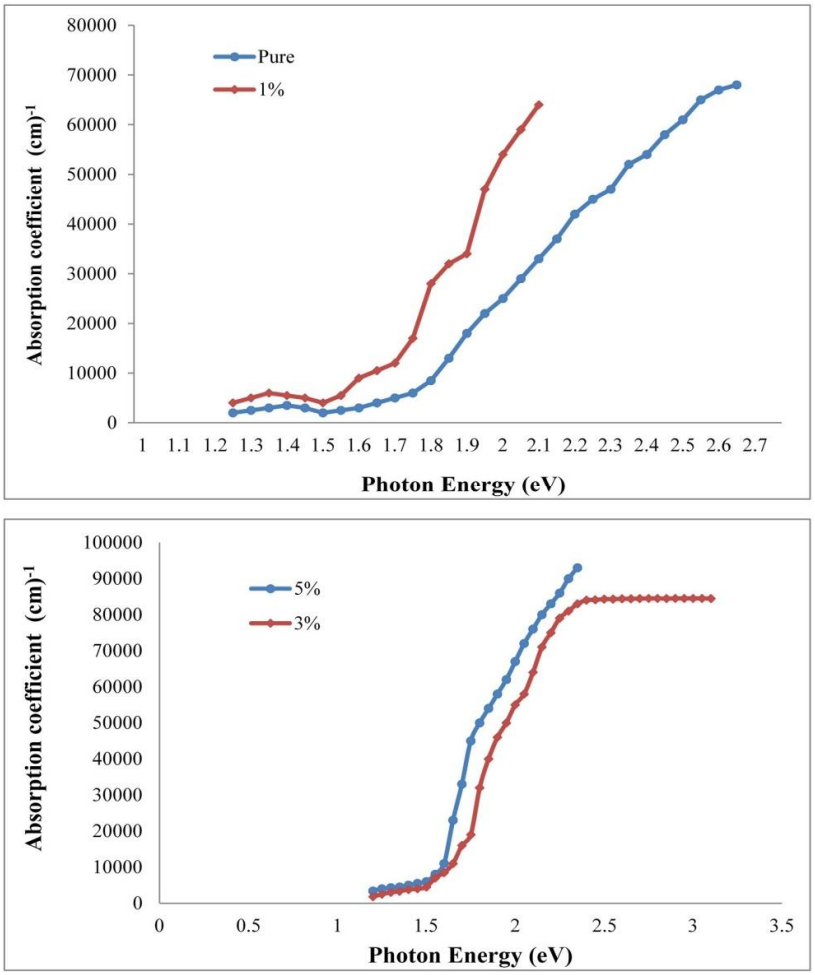


**Fig. 10. The absorption coefficient as a function of photon energy at different Cu wt%**

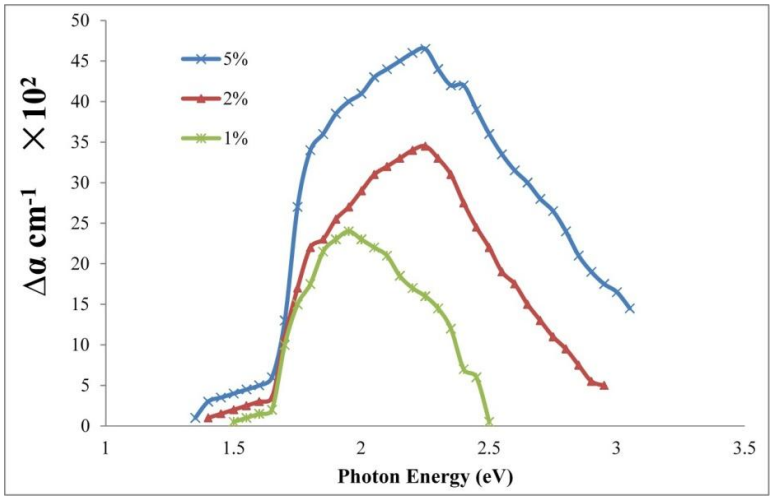


**Fig. 11. The change in absorption coefficient for various doping concentrations as a function of photon energies**

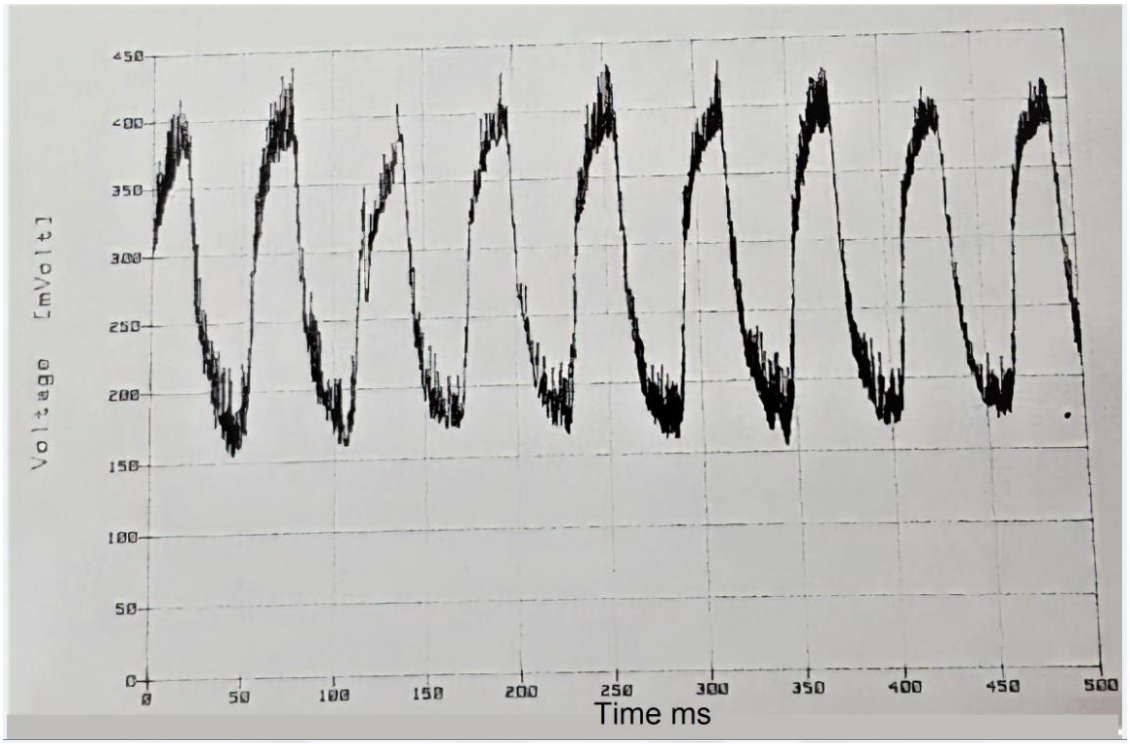


**Fig. 12. The output signal of the modulated $CO_2$ Laser**

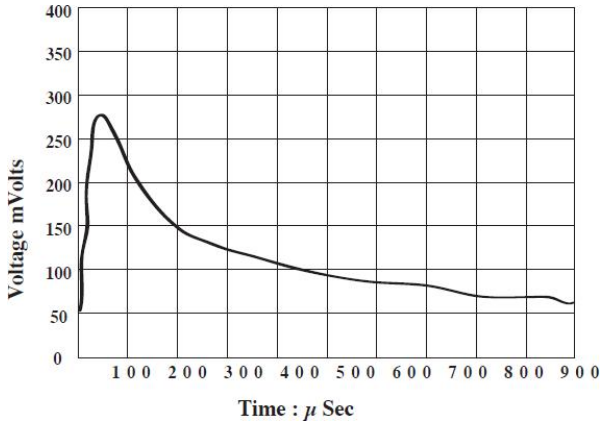


**Fig. 13. The output signal of the GaAs semiconductor laser**

Fig. 14a depicts the energy levels involved in the absorption of CdSe:Cu film. This schematic diagram shows a wide wavelength tuning range extending from the visible to the infrared spectrum. This tuning spectrum of the copper doped bulk CdSe can be compared with colloidal CdSe-ZnS core-shell quantum dots (Fig. 14b). The common index of the bulk CdSe:Cu and the colloidal CdSe core-shell quantum dots is the single crystalline structure. As a matter of fact, the bulk crystal covers the micorscale range, whereas the quantum dots is in the nanoscale. However, this tuning spectrum was detected by using a surface Plasmon's technique. Five distinguishable transitions were detected by the absorption and fluorescence spectra of the CdSe quantum dots [21]. The populations of these levels were explained by the multiple exciton generation (MEG), in full agreement with the theoretical predictions. It can be remarked that the traditional bulk CdSe doped Cu and the CdSe –ZnS quantum dots are manifested in wavelength tuning. The advantages of the bulk CdSe over the size dependent

confinement energy of the same semiconductor material are easier to prepare and at much less fabrication cost than the corresponding size confinement quantum dots. Besides, the CdSe quantum dots tuning range never extends over the visible region of the spectrum, whereas this reported tuning of the bulk CdSe:Cu does extend to the infrared region. Recently, researches were done in the synthesis and characterization of CdSe doped Cu nanoparticles. Raj et al. [22] were observed that the increase in the concentration of copper shifts the emission towards the higher wavelength. They explained such blue shift was caused by strong confinement effect. Meulenberg et al. [23] have studied the structure and composition of Cu doped CdSe nanocrystals using soft X-ray absorption near edge spectroscopy (XANES). They indicated changes in the Se density of states with Cu doping, due to a local bonding environmental effect. Bear et al. [24] have studied copper doped CdSe-ZnS core-shell quantum dots (QD) and have shown that doping small amounts of Cu into the ZnS shell partially quenches the QD core luminescence and a blue shift in luminescence peak with respect to pure ZnS shell was detected. This is in contrast to a pure ZnS shell, where a significant increase in quantum yield and a red shift in luminescence were observed. The pioneer work of Türe et al. [25] have investigated by photoconductivity and space-charge region capacitance technique multiple levels of copper centers in single crystal of CdSe. They demonstrated that the only center referring to copper was situated at 1eV with respect to the valence band. Photoluminescence blinking dynamics for $Cu^{+}$:CdSe was analyzed by Whitham et al. [26] and compared to undoped CdSe nanocrystal. They identified the effect of $Cu^{+}$, which selectively traps photogenerated holes and revealed that the $Cu^{+}$:CdSe nanocrystal off state dynamics are statistically identical. A theoretical and experimental studies implemented by Wright and Meulenberg [27] have demonstrated the effect of dopant into the CdSe quantum dots. They predicted that the dopant concentration causes a lowering of band energy as compared to the bulk band gap energy (1.73 eV). This red shift was explained in terms of the contribution of both the hybridization energy and the confinement energy. They demonstrated that the dopant can affect not only the electronic structure but also the optical properties.

It can be concluded from the previous studies in CdSe:Cu as a bulk or a nanostructure, no evidences were reported for the existence of Cu localized levels with an accurate determination of their positions in the band gap of CdSe, particularly, in the infrared region of the spectrum.

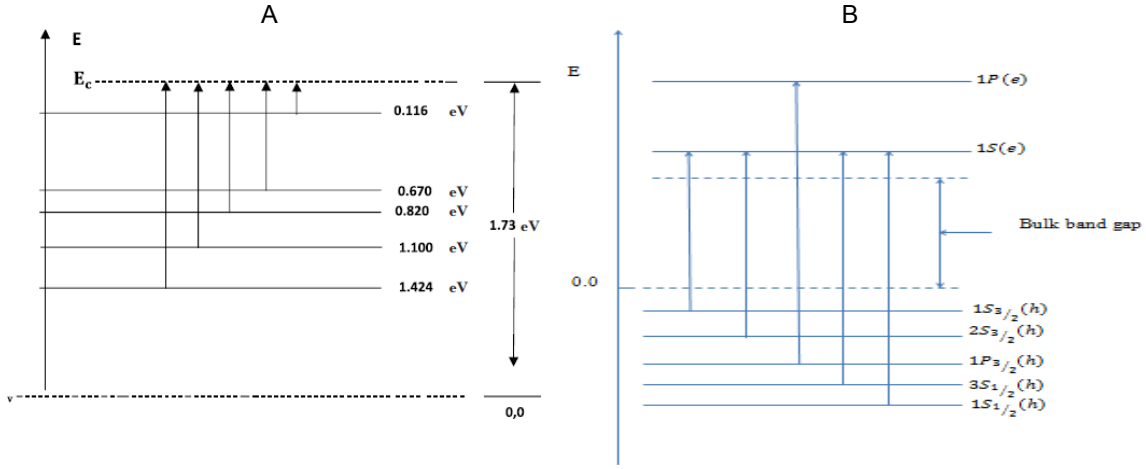


**Fig. 14. A) Energy levels involved in the absorption of CdSe:Cu film B) Energy levels involved in the absorption and fluorescence of CdSe-ZnS core-shell quantum dots [21]**

## 4.4 Detection Characteristics

Fig. 15 shows that the photoconductivity of the CdSe grows exponentially with the increase in Cu wt% concentration. This growth feature is due to the improvement of the film structure. This improvement is confirmed by the increase in the crystal grain size as stated earlier. The noise voltage and the responsivity of this detector are measured and found to be ~1nV and 0.73V/W respectively. The detectivity was calculated by using the following relationship:

$$D^* = (A\,\Delta f)^{1/2}\, R / V_n \quad (7)$$

Where A is the detector active area (A=0.1 $cm^2$), (Δf=1Hz) the electrical bandwidth, $V_n$ is the noise voltage and R is the responsivity. Using the Eq.1, a value of $D^*=2.31\times10^8$ cm $Hz^{1/2}W^{-1}$ is obtained. The comparison of this D* value of the CdSe bulk detector at room temperature with the specific detectivity across a different technology is reasonable. The room temperature detectivity of the state of art MCT is $2\times10^8$ cm $Hz^{1/2}W^{-1}$[28] which approaches the measured D* value for the CdSe:Cu detector. However, the predicted detectivity can be increased by an optimization methodology which includes surface plasmons effect by deposition of the CdSe films into gold coated substrates. Besides, other dopant than Cu like Ag and Au can be used for comparison. The present CdSe:Cu detector paves the way for further investigations and improvements in the field of a dual range antiaircraft missile seekers and may be other applications.

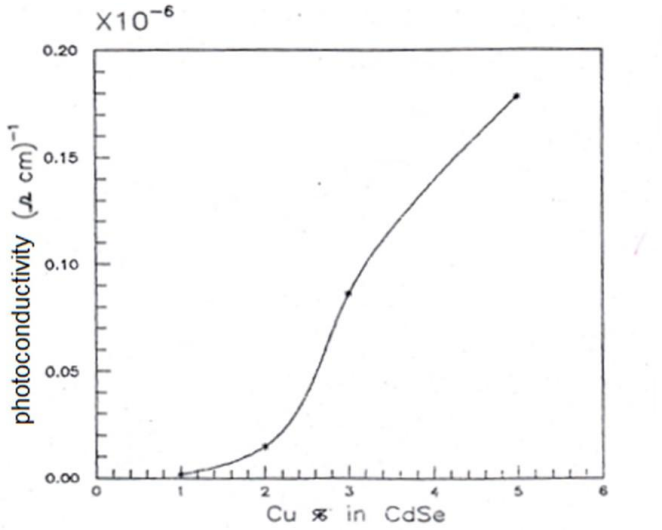


**Fig. 15. The photoconductivity of CdSe as a function of Cu wt% concentration**

## 5. CONCLUSIONS

The following conclusions are drawn:

(i) The tuning range of the bulk CdSe:Cu is found greater than the recent technological CdSe quantum dots. This may open the door for more applications, particularly in the IR region of the electromagnetic spectrum.
(ii) The detectivity of this detector at room temperature is comparable with the corresponding state of art MCT detector and the recent designed GaN QDs. Therefore, the CdSe:Cu detector can be considered as an additional prototype to the traditional MCT as an IR detector operating at room temperature.

## COMPETING INTERESTS

Authors have declared that no competing interests exist.

## REFERENCES

1. Zhang J, Itzler MA, Zbinten H, Pan JW. Advances in InGaAs/InP single- photon detector systems for quantum communications. Light Science and Applications. 2015;4:e286. Available:http://dx.doi.org/10.1038/ lsa.2015.59
2. Maiti A, Bhattacharyya S. Quantum dots and applications in medical science. International Journal of Chemical Science and Chemical Engineering. 2013;3(2):37-42. Available:http://www.r.publication.com

3. Kashyout AB, Soliman HMA, Fathy M, Goma EA, Zidan AA. CdSe Quantum dots for solar cells devices. International Journal of Photoenergy. 2012;1-7.
   Available:http://dx.doi.org/10.1155/2012/952610
4. Oertel DC, Bawendi MG, Arango AC, Bulovic V. Photodetector based on treated CdSe quantum dots films. Applied Physics Letters. 2005;87(21):213505.
   Available:http://dx.doi.org/10.1063/1.2136227
5. Asgari A, Razi S. High performances III-nitride quantum dot infrared photodetector operating at room temperature. Optics Express. 2010;18(14):14604-14615.
6. Diedenhofen SLD, Kufer D, Lasanta T, Konstantatos G. Integrated colloidal quantum dot with color-tunable plasmonicnanofocussing lenses. Light Science Applications. 2015;4:e234.
   Available:http://dx.doi.org/1038/ Isa.2015.7
7. Wageh S, Al-Ghamdi AA, Al-ZahraniAA, Driss H. High quantum yield Cu doped CdSe quantum dots. Mater. Res. Express. 2019;6:0850d4.
   Available:http://doi.org/10.1088/2053-1591/ab268f
8. Cakmakyapan S,Lu PK, Novabi A, Jarrahi M. Gold-patched graphene nano-stripes for high-responsivity and ultrafast photodetection from the visible to infrared regime. Light: Science & Applications. 2018;7:20.
   DOI: 10.1038/s41377-018-0020-2
9. Yang D, Ma Dongge. Development of organic semiconductor photodetectors: From mechanism to applications. Advanved Optical Materials. 2019;7:1800522.
   DOI: 10.1002/adom.201800522
10. Mei F, Sun D, Mei S, Feng J, Zhou Y, Xu J, Xiao X. Recent progress in perovskite-based photodetectors: The design of materials and structures. Advances in Physics: X. 2019;4(1): 1592709.
    Available:http://doi.org/10.1080/23746149.2019.1592709
11. Sze SM, Ng KK. Physics of semiconductor devices. Wiley- Interscience; 2007.
12. Dereniak EL, BoremanGD. Infrared detectors and systems. John Wiley & Sons, New York; 1996.
13. Mohammed HH, AL-Ani SKJ. The fabrication of the infrared CdSedopped with Cu photodertector. Applied Physics Research. 2016;8(3):96-103.
    Available:http://dx.doi.org/10.5539/apr.v8n3p96
14. Glew RW. Cadmium selenide sputtered films. Thin Solid Films. 1977;46:59-67.
15. Metha RR, Sharma BS. Photoconductive gain greater than unity in CdSe films with Shottky barriers at the contacts. J. Appl. Phys. 1973;44:352-328.
16. Kainthi RC, Panadya DK, Chopra KL. Photoelectronic properties of solution grown CdSe films. Solid State Electr. 1982;25:73-76.
17. Türe IE, Ressell GJ, Woods J. Photoconductivity, structure and defect levels in CdSe crystals. J. Cryst. Growth. 1982;59:223-228.
18. Mohammed HH, AL-Ani SKJ, AL-Ani SGK. Optical, electrical and detector properties of polycrystalline films of CdS doped with Cu.Iraqi J. Sci. 2000;41(4):227-242.
19. AL-Ani SKJ, Mohammed HH, Al-Fwade EMN. The optoelectronic properties of CdSe: Cu photoconductive detector. Renewable Energy. 2002;25:585-590.
20. Wei SH, Zhang SB, Zunger A. First-principles calculation of band offset, optical bowings, and defects in CdS, CdSe, CdTe, and their alloys. Journal of Applied Physics. 2000;87(3):1304-1311.
    Available:http://scitation.aip.org/termsconditions
21. Mohammed HH. CdSe-ZnS core-shell quantum dots: Surface plasmons effect and optical spectra. Applied Physics Research. 2013;5(6):15-22.
    Available:http://dx.doi.org/10.5539/apr.v5n6p15
22. Raj DJV, Linet JM, Das SJ. Synthesis and characterization of 1- thioglycerol capped CdSe and Cu (copper) doped CdSe nanoparticles at room temperature. International Journal of ChemTech Research. 2014;6(3):2042-2044.
    Available:http://www.sphinxsai.com/framesphinxsaichemtech.htm

23. Meulenberg RW, Buuren TV, Hanif KM, Strouse GF, Terminello L. Structure and composition of Cu-doped CdSe nanocrystals using soft X-ray absorption spectroscopy. Nano Letters. 2004; 4(11):2277-2285.
24. Bear JC, Hollingsworth N, McNaughter PD, Mayes AG, Ward MB, Nann T, Parkin IP. Copper - doped CdSe/ZnSquantum dots: Controllable photoactivated copper (I) cation storage and release vectors for catalysis. AngewandteChemie International Edition. 2014;53(6):1598-1601. Available:http://dx.doi.org/10.1002/anie.2013308778
25. Türe IE, Claybourn M, Brinkman AW, Woods J. Copper centers in CdSe. J. Appl. Phys. 1986; 60(5):1670-1675. Available:http:// dx.doi.org/10.1063/1.337256
26. Whitham PJ, Knowles KE, Raid PG, Gamelin DG. Photolumiescence blinking and reversible electron trapping in copper-doped CdSe nanocrystal. Nano Lett. 2015;15(6):4045-4051. Available:http://dx.doi.org/10.1021/acs.nanolett.5b01046
27. Wright TW, Meulenberg RW. Effects of dopants on the band structure of quantum dots: A theoretical and experimental study. Physical Review B. 2013;88:045432-1-8. Available:http:// dx.doi.org/10.1103/Phys Rev B.88.045432
28. Hamamatsu. Infrared detectors, Selection Guide-March; 2015. Available:http://www.hamamatsu.com/ resources/pdf/ssd/ingaos_kird0005epdf

**Biography of author(s)**

**Professor Hassan H. Mohammed**
Department of Computer Engineering Technology, Iraq University College, Alestiqlal Street, Basrah, Iraq.

He was born in Basrah city, the first of July 1951. He has a B.Sc. degree in physics from the Basrah University (honor) in 1972, M.Sc. degree in (molecular physics) in 1975, DEA and obtained the Ph.D. degree from the University of Paris 11 (Orsay), France in 1981. The thesis was in the field of (matrix isolation optical spectroscopy using laser sources). The fields of interests are: lasers in spectroscopy, lasers in medicine, nanotechnology, photodetectors, optical communications and tracking and philosophy of physics. He worked as a lecturer and research staff at the University of technology and chief researchers and head of lasers and optoelectronics center at the Ministry of Science and Technology (MOST), Baghdad. In 2008 he joined the University of Basrah, physics department and worked as an assistant professor first and then as a full professor in physics. At present he connected with the Iraq University college, department of technical computer engineering as a lecturer and research staff. He has published 40 articles, supervised 36 M.Sc. and Ph.D. theses during the research period, 2 published books and also has 4 patents in applied physics field. He awarded the medal of scientists in Iraq for his contribution in scientific researches. E-Mail: dr.hassanh50@gmail.com

**Professor Salwan K. J. Al-Ani, Ph.D.**
Department of Physics, College of Science, Al-Mustansiriya University, Baghdad, Iraq.

He holds a Ph.D. degree in Physics from the Brunel University, U.K. in 1984, a Master degree in Theoretical Physics from Surrey University, U.K. in 1981 and a B.Sc. degree in Physics from Baghdad University, Iraq in 1977. He became a Professor of Physics at Baghdad University in 1994. He received the award "*Shoman Prizes* "for Young Arab Scientists for Physics and

Geology"(Jordan) in 1993. In 1998 he was honored as a "Scientist" group (A) in Physics according to the Scientists Welfare Law, No. (1) 1993 and its instructions in No. (10) 1998 (IRAQ). Heholds five patents in the optoelectronic devices of non-crystalline and amorphous materials and had supervised more than 50 Ph.D. and M.Sc. theses in Physics. He has Published 200 scientific archival in international refereed journals and published several scientific books in the field of Physics. He served as an Editor in Chief and a Reviewer to many international Journals. He held several senior academic and administrative positions, including a Dean of a Faculty of Science Baghdad University (1998-2000). Later he has been appointed the Dean of a Faculty of Education – Hadramout University in Yemen (2003-2007). Presently he is working at the State of Qatar. Email:salwan_kamal@yahoo.com, profdrsalwanalani@gmail.com



**DISCLAIMER**
This chapter is an extended version of the article published by the same author(s) in the following journal.
Applied Physics Research, 8(3), 2016.